Dyes and Pigments 107 (2014) 127–132

Contents lists available at ScienceDirect

Dyes and Pigments

journal homepage: www.elsevier.com/locate/dyepig

A sensitive and selective fluorescence probe based fluorescein for detection of hypochlorous acid and its application for biological imaging

Wenzhu Yin [a], Hongjun Zhu [a,*], Ruiyong Wang [b]

[a] Department of Applied Chemistry, College of Science, Nanjing Tech University, Nanjing 211816, PR China
[b] School of Life Science, Nanjing University, Han Kou Road 22, Nanjing, Jiangsu 210093, PR China

ARTICLE INFO

Article history:
Received 11 February 2014
Received in revised form
9 March 2014
Accepted 10 March 2014
Available online 27 March 2014

Keywords:
Fluorescein
Hypochlorite anion
Biological imaging
Water solubility
Flourescent probe
Spirolactam

ABSTRACT

A highly sensitive and selective fluorescein-based probe **1** for hypochlorite anion was synthesized. The probe **1** has favorable characteristics for biological imaging, including high water solubility, high fluorescence yield, pH-independent fluorescence, and biocompatibility. Results show that it has a detection limit of 40 nM to hypochlorite anion. In addition, confocal fluorescence microscopy imaging using RAW264.7 cells showed that the new probe **1** could be used as an effective fluorescent probe for detecting HOCl in living cells.

1. Introduction

Hypochlorite anion (ClO^-) is one of the biologically important reactive oxygen species (ROS), and produces in organisms by the reaction of H_2O_2 with Cl^- ions under the catalysis of a heme enzyme, myeloperoxidase [1,2]. Endogenous ClO^- is essential to life and has important antibacterial properties. However, excessive or misplaced production of ClO^- can lead to tissue damage and diseases, such as atherosclerosis, arthritis, and cancers [3]. Therefore, real-time monitoring and accurate detection of ClO^- anion are attracting increasing attention due to its extremely important role in health and environmental science. Fluorescent probes possess some native advantages over the probes of other types because of their high sensitivity, specificity, simplicity of implementation, and fast response times, offering application methods for not only in vitro assays but also in vivo imaging studies [4–8]. So far, a number of small-molecule fluorescent probes for specific detection of HOCl/OCl^- have been reported [9–21]. However, some of them still face some drawbacks, such as poor water-selectivity, low sensitivity, and pH dependency [22]. Therefore, it is highly desirable to develop new fluorescent probes that can overcome these limitations in detecting HOCl/OCl^-. The fluorescein framework seems to be an ideal model to construct "turn-on" fluorescent chemosensors due to its favorable properties such as excitation and emission wavelengths in the visible region with a high fluorescence quantum yield [23–26], easy synthesis and functionalization [27], excellent biocompatibility and cellular membrane-penetrating capacity [28–31]. With these considerations in mind, we synthesized a new fluorescein-based chemosensor bearing a catechol moiety which responded to the amount of ClO^- for detection of hypochlorite anion (Scheme 1). Being a closed spirolactam structure, the probe itself was nearly nonfluorescent, while the strong green fluorescence was restored after addition of HClO. It was ascribed to the opening ring of spirolactam via oxidation of catechol moiety by HClO and then hydrolysis of diacylhydrazine [32]. The probe display highly sensitive and selective detection toward ClO^- over other ROS or reactive nitrogen species (RNS).

2. Experimental

2.1. Materials

Unless otherwise stated all chemicals were commercially obtained and used without further purification. NaOCl was purchased

* Corresponding author. Tel.: +86 25 83172358; fax: +86 25 83587428.
E-mail addresses: zhuhj@njtech.edu.cn, zhuhjnjut@hotmail.com (H. Zhu).

http://dx.doi.org/10.1016/j.dyepig.2014.03.012
0143-7208/

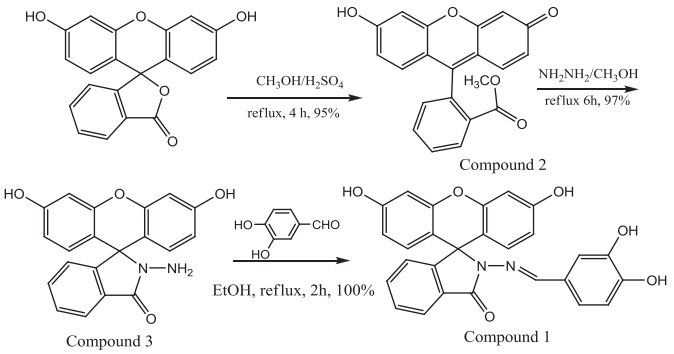

Scheme 1. The routes of synthesis of compound 1.

from Sinopharm Chemical Reagent Co., Ltd (China) and the concentration was determined by titration with $Na_2S_2O_3$.

2.2. Measurements

The UV–vis spectra were recorded on a Perkin Elmer Lambda 35 spectrophotometer. Fluorescence measurements were performed at room temperature on a Perkin Elmer LS-55 spectrophotometer or Hitachi Fluorescence spectrophotometer-F-4600, and Fluorescein was used as a standard for the determination of fluorescence quantum yields. The biological imaging tests were carried out with an Olympus FV-1000 and Leica TCS-SP5 laser scanning confocal fluorescence microscopes. ^{1}H NMR and ^{13}C NMR were measured on a Bruker AV-300 spectrometer with chemical shifts reported in ppm (in DMSO-d_6 or $CDCl_3$, TMS as internal standard). Mass spectra were recorded using a Thermo Finnigan LCQ Duo electrospray mass spectrometer in positive ion mode by direct infusion, with spray voltage 4.5 kV and capillary temperature of 200 °C.

2.3. Synthesis of compound **1** (probe **1**)

As shown in Scheme 1, the probe **1** (compound **1**) was readily synthesized by treating fluorescein with methanol using H_2SO_4 as catalyst, which was followed by hydrazine hydrate and 3,4-dihyrdoxybenzaldehyde. The structure of probe **1** was confirmed by ^{1}H NMR, ^{13}C NMR, ESI-MS. Compound 2 and 3 were synthesized according to our previous procedures [33].

2.3.1. Synthesis of compound **2**

To fluorescein (1.0 g, 3.1 mmol) methanol solution (10 mL) in a 25 mL round-bottom flask, was added concentrated sulfuric acid (98%) (1 mL). The solution was refluxed and stirred for 4 h. After cooling, excess methanol was removed under reduced pressure and excess water was added to the residue. The red solid formed was washed with water several times and filtered in vacuum until almost free from fluorescence. After dried in vacuum, 0.95 g red solid fluorescein methyl ester **2** was obtained with a yield of 91%. M.p.: 212–214 °C; ^{1}H NMR ($CDCl_3$, 300 MHz) δ (ppm): 8.31 (d, 1H, J = 7.8 Hz), 7.79 (m, 2H), 7.34 (d, 1H, J = 7.2 Hz), 7.28 (d, 2H, J = 3.6 Hz), 7.19 (d, 2H, J = 9.0 Hz), 7.08 (dd, 2H, J_1 = 9.3 Hz, J_2 = 2.1 Hz), 3.63 (s, 3H).

2.3.2. Synthesis of compound 3

Compound **2** (0.40 g) and hydrazine hydrate (0.24 g, 4.8 mmol) were added to methanol (5 mL), refluxed and stirred for 6 h. After collecting by filtration, the light brown precipitate was washed by a small amount of methanol and water. 0.41 g straw yellow fluorescein hydrazone **3** was dried in vacuum and then obtained with a yield of 98%. M.p.: 252–253 °C; ^{1}H NMR (DMSO-d_6, 300 MHz) δ (ppm): 7.77 (t, 1H, J = 4.8 Hz), 7.49 (t, 2H, J = 3.6 Hz), 6.98 (m, 1H), 6.59 (d, 2H, J = 2.1 Hz), 6.42 (m, 4H), 4.38 (s, 2H).

2.3.3. Synthesis of compound **1**

Compound **3** (346 mg, 1.0 mmol) was dissolved in absolute methanol (20 mL). 3,4-dihydroxybenzalhyde (138 mg, 1.0 mmol) was added and the mixture was heated at reflux for 4 h. The precipitate produced was filtered and washed with cold ethanol. The crude product was purified by recrystallization from ethanol to afford **1** as brown solid (420 mg, 90%). M.p.: >300 °C (dec); ^{1}H NMR (300 MHz, DMSO-d_6) δ (ppm): 9.88 (s, 2H), 9.39 (s, 1H), 9.18 (s, 1H), 8.76 (s, 1H), 7.86 (dd, J = 6.1, 2.2 Hz, 1H), 7.64–7.47 (m, 2H), 7.06 (dd, J = 5.9, 1.8 Hz, 1H), 6.87 (s, 1H), 6.70–6.58 (m, 4H), 6.45 (m, 4H). ^{13}C NMR (75 MHz, DMSO-d_6), δ 163.32, 158.42, 152.03, 150.85, 150.70, 148.34, 145.56, 133.60, 128.98, 128.90, 127.95, 125.71, 123.53, 122.96, 120.70, 115.46, 112.29, 112.25, 110.21, 102.45, 65.07. ESI-MS (-p) (m/z): 465.75 ($[M-H]^-$), 501.58 ($[M+2H_2O-H]^-$), 525.33 ($[M+CH_3CO_2H-H]^-$), 931.25 ($[2M-H]^-$)

2.4. Determination of quantum yield

The fluorescence quantum yields were determined using fluorescein as a reference with a known Φ value of 0.89 in EtOH [34]. The sample and the reference were excited at the same wavelength (λ_{ex} = 480 nm), maintaining nearly equal absorbance (0.06). The quantum yield was calculated according to the following eqn (1):

$$\Phi_S/\Phi_R = (A_S/A_R) \times (Abs_R/Abs_S) \times \left(\eta_S^2/\eta_R^2\right), \quad (1)$$

where Φ_S and Φ_R are the fluorescence quantum yields of the sample and the reference, respectively; A_S and A_R are the emission areas of the sample and the reference, respectively; Abs_S and Abs_R are the corresponding absorbance of the sample and the reference solution at the wavelength of excitation; η_S and η_R are the refractive indices of the sample and the reference, respectively.

2.5. Cell culture

RAW264.7 macrophages were first incubated with LPS (1 μg/mL) and IFN-γ (50 ng/mL) in culture medium for 4.5 h at 37 °C, and then were stimulated with PMA (10 nM) for 45 min at 37 °C. Subsequently, part of the treated cells was incubated with L-methionine (300 μM) for 40 min at 37 °C. After washed with PBS buffer (0.10 M, pH 7.4) for three times, all the cells were incubated with probe **1** (10 μM) in culture medium for 30 min at 37 °C. Before imaging, the cells were washed again with PBS (0.10 M, pH 7.4) for three times.

3. Results and discussion

3.1. Selectivity studies

To evaluate whether probe 1 can selectively respond to OCl^- under simulated physiological conditions (pH = 7.4), the fluorescence responses of probe 1 to other potentially competing ROS/RNS, were also performed. As shown in the selectivity profiles (Fig. 1), only OCl^- incurs a dramatic fluorescence enhancement for probe 1. Other ROS or RNS, including H_2O_2, t-BuOOH, NO_2^-, NO_3^-, and $S_2O_8^{2-}$, exert no obvious spectral changes.

In addition, probe **1** was treated with a wide variety of cations and anions to examine the selectivity. As shown in Fig. 3, the addition of ClO^- induced a significant redshift of the fluorescence emission spectra. However, representative species such as Li^+, Na^+, K^+, Mg^{2+}, Ca^{2+}, Zn^{2+}, Cu^{2+}, Al^{3+}, Cl^-, CH_3COO^-, SO_4^{2-}, CO_3^{2-}, elicited almost no changes in the fluorescence spectra. Furthermore, the

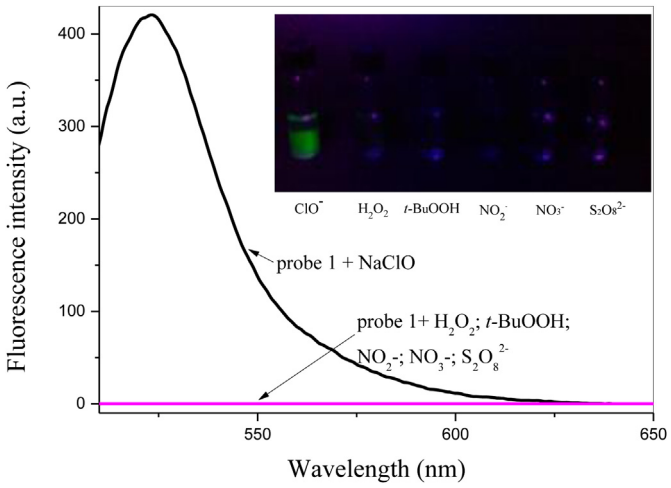

Fig. 1. Fluorescence changes of probe **1** (2 μM) in response to NaOCl (20 μM) and various ROS/RNS (20 μM) in a H_2O/DMSO (v/v = 20/1, Tris–HCl buffer, 0.05 M, pH 7.4) solution. The excitation wavelength was 490 nm. Inset: Fluorescence response of probe **1** (2 μM) to 10 equiv of various ROS/RNS in a H_2O/DMSO (v/v = 20/1, Tris–HCl buffer, 0.05 M, pH 7.4) solution.

visual fluorescence response of probe 1 to various species (Fig. 2) demonstrates that the probe can be used conveniently for hypochlorite detection by simple visual detection.

3.2. UV absorption response of probe *1* to OCl^-

The absorption spectra of probe **1** in the absence and presence of different amounts of OCl^- are shown in Fig. 3. Probe **1** only exhibited an absorption peak centered at 338 nm, which was ascribed to the absorption of xanthene moiety. Meanwhile, there was almost no typical ring-opened spirolactam absorption in the 496 nm region. Upon addition of increasing concentrations of OCl^-, absorption peak at 496 nm enhanced significantly, indicating that the OCl^- promoted ring opening of spirolactam in the fluorescein moiety, while the absorption of xanthene moiety at 338 nm red-shifts to 368 nm with the peak intensity decreasing gradually. During the titration a beautiful UV–visible spectral pattern was

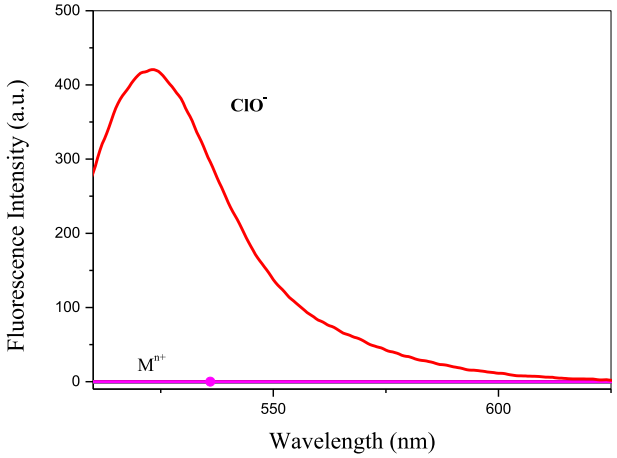

Fig. 2. The fluorescence spectra of **1** (10 μM) upon addition of 5 equiv of various metal ions including of Li^+, Na^+, K^+, Mg^{2+}, Ca^{2+}, Zn^{2+}, Cd^{2+}, Hg^{2+}, Pb^{2+}, Mn^{2+}, Cu^{2+}, Ag^+, Fe^{2+}, Fe^{3+}, Co^{2+}, and Ni^{2+} in a H_2O/DMSO (v/v = 20/1, Tris–HCl buffer, 0.05 M, pH 7.4) solution. Inset: Fluorescence response of **1** (10 μM) to 5 equiv of various metal ions in a H_2O/DMSO (v/v = 20/1, Tris–HCl buffer, 0.05 M, pH 7.4) solution.

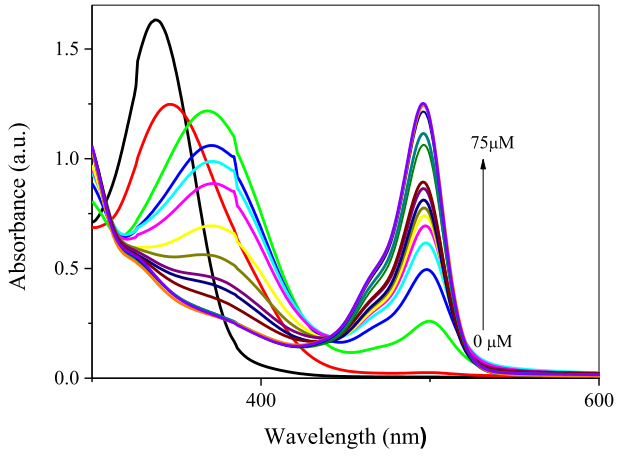

Fig. 3. Changes in absorption spectra of probe 1 (5 μM) in a H_2O/DMSO (v/v = 20/1, Tris–HCl buffer, 0.05 M, pH 7.4) solution with various amount of OCl^- (0–75 μM).

observed with an isosbestic point at 440 nm, which indicated formation of a new unique compound. At this stage, the color of solution became yellowish green from colorless and the absorbance at 496 nm reached max when the addition of 15 equiv of NaClO. These results indicated that probe 1 can be used as a "naked-eye monitor" for detection of HClO.

3.3. Fluorescent response of probe *1* to OCl^-

In order to evaluate the sensitivity of probe 1 to OCl^- in a Tris–HCl buffer solution (pH = 7.4), fluorescence titration were carried out. Addition of NaOCl (aq) to the solution of the probe **1** caused an immediate, strong change in fluorescence intensity with a new band centered at 523 nm formed under 490 nm excitation wavelength (Fig. 4). The emission intensity reached its maximum after the addition of 15 equiv of HOCl. The quantum yield of the probe **1** with NaClO was $\Phi = 0.87$, which is 1240-fold higher than that of **1**, at $\Phi = 0.0007$. Notably, there was a good linear correlation between the fluorescence intensity and the concentration of NaOCl (0–1.0 μM, $R^2 = 0.9989$) (seeing Supporting information, Fig. S1). Furthermore, it was found that **1** has a detection limit of 40 nM, on the basis of the signal-to-noise ratio (S/N = 3), which makes it sufficiently sensitive for application in living systems. Thus, probe 1

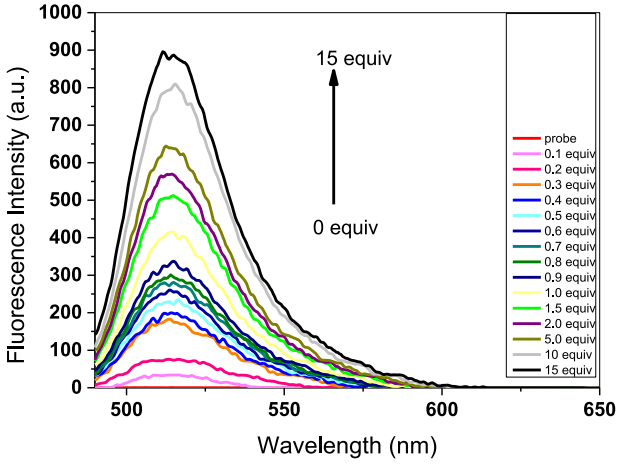

Fig. 4. Fluorescence changes of probe **1** (5 μM) in the presence of various equivalents of NaOCl (0–15 equiv) in a H_2O/DMSO (v/v = 20/1, Tris–HCl buffer, 0.05 M, pH 7.4) solution. The excitation wavelength was 490 nm.

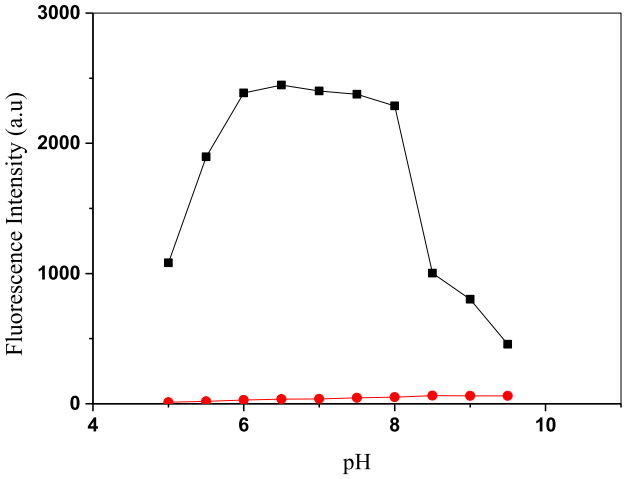

Fig. 5. Fluorescence intensity of probe **1** (10 μM) at various pH values in a H_2O/DMSO (v/v = 20/1, Tris–HCl buffer, 0.05 M, pH 7.4) solution in the absence and presence of ClO^- (2 equiv) (excitation at 490 nm, emission at 517 nm, emission slit 5 nm).

appears to be highly sensitive and selective for the detection of HOCl. Moreover, it is worth noting that probe 1 can rapidly respond to NaOCl within seconds, making it a good candidate for real-time detection of hypochlorite generation.

3.4. The effect of pH on the fluorescence

To essay the practical application of probe **1** in the detection of HOCl (pKa = 7.6), the pH dependence of the photophysical properties of **1** was investigated in a series of Tris–HCl buffers with different pH values ranging from 5 to 9 (Fig. 5).

The probe in Tris–HCl buffer (pH 5–9.5) exhibits almost no emission when excited at 490 nm and no distinct variations are observed after 24 h, suggesting that probe **1** is stable under the measurement condition. Fig. 5 indicted that the probe **1** is capable of selectively detecting hypochlorite without interference by other biological ROS in pH variations (5–9.5). Probe **1** itself were essentially pH-insensitive across a wide range of pH values. However, the fluorescent responses to the probe **1** towards NaOCl was pH-dependent; the maximal sensing responses of probe **1** upon treatment with 2 equiv of NaOCl was observed at pH 6.0–8.0 (pKa of HOCl is 7.6), suggesting that the assay is compatible with most biological applications (pH = 7.4).

3.5. Biological applications

Probe **1** is well-suited to fluorescence imaging in living cells. As determined by laser scanning confocal microscopy imaging experiments (Fig. 6), staining RAW264.7 macrophages cells with 10 μM probe **1** at 37 °C for 30 min exhibited faint fluorescence in the optical window 490–550 nm with 488 nm exited wavelength (Fig. 6(a)). Treating the cells with 10 μM NaOCl for 10 min led to remarkable fluorescence enhancement (Fig. 6(b)), indicating that probe **1** is extremely sensitive for detecting exogenous OCl^- in living cells. These cells kept well their morphologies, and suggested that probe **1** do not exhibit marked cytotoxicity in our experimental conditions.

The images of cells were obtained using a confocal fluorescence microscope. As shown in Fig. 6(a), when RAW264.7 cells were incubated with probe **1** (10 μM), no fluorescence was observed in the RAW264.7 cells (Fig. 6(b)). After the treatment with NaOCl, yellow-green fluorescence was observed in the RAW264.7 cells

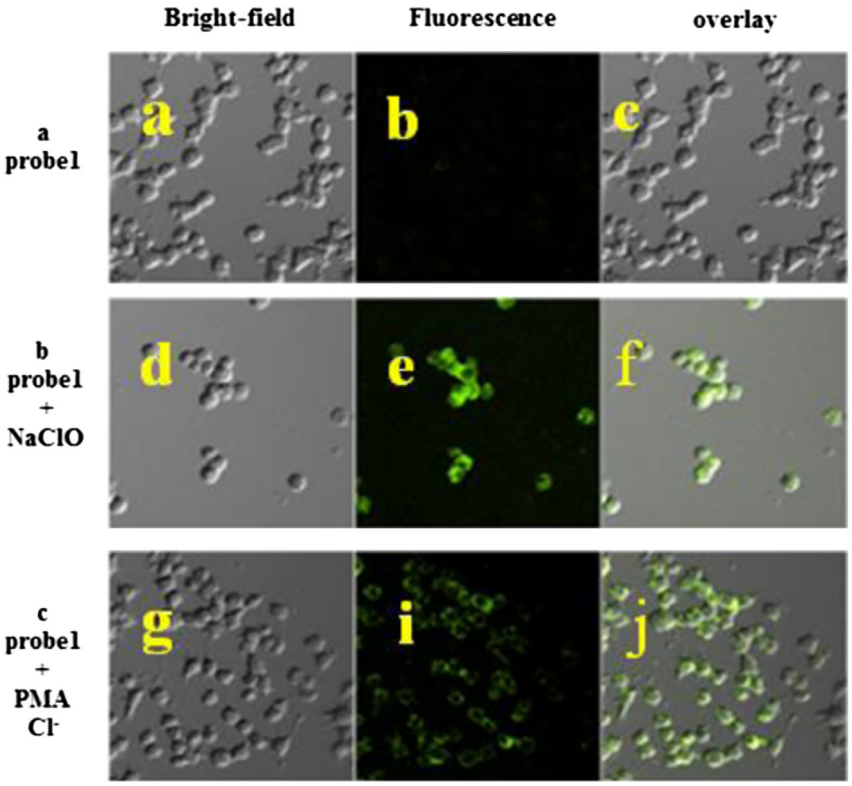

Fig. 6. Fluorescence images of RAW264.7 cells. (Left) fluorescence image; (Middle) Bright-field image and (Right) overlay image. (a) The cells incubated with probe **1** (10 μM) for 30 min. (b) Subsequent treatment of the cells with NaOCl (10 μM) for 10 min. (c) The cells treated with stimulant PMA (25 ng/mL) for 2 h in the presence of for 30 min. (λ_{ex} = 488 nm, λ_{em} = 490–550 nm).

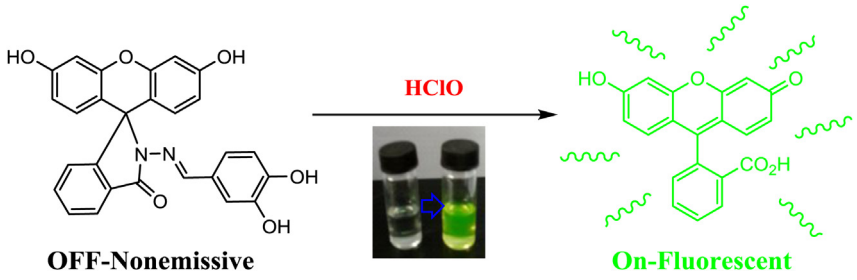

Scheme 2. Turn-on sensing of HOCl via HOCl-promoted probe 1 oxidation reaction (photos show fluorescence of probe 1 in a H_2O/DMSO (v/v = 20/1, Tris–HCl buffer, 0.05 M, pH 7.4) solution).

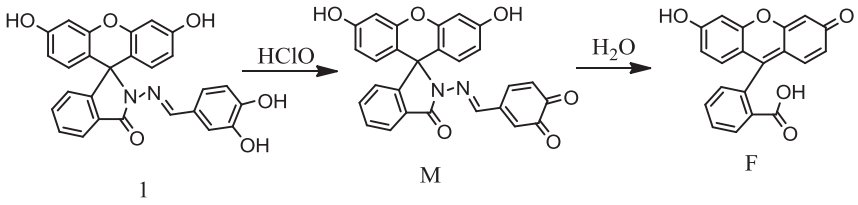

Scheme 3. Proposed mechanism for the reaction of probe **1** with HOCl.

(Fig. 6(e)). An overlay of fluorescence and bright-field images (Fig. 6(f)) show that the fluorescence signals are localized in the intracellular area, indicating a subcellular distribution of HOCl and the good cell-membrane permeability of probe **1**.

Encouraged by these results as demonstrated above, we further evaluated whether the probe **1** could be used to monitor endogenous hypochlorite in living cells. Macrophages and other phagocytic cells are known to produce low micromolar levels of H_2O_2 or other ROS during phagocytosis, or when stimulated by agents such as phorbol myristate acetate (PMA) [35–37]. RAW264.7 macrophages were treated with PMA (25 ng/mL) for 2 h, after which the cells were incubated with probe **1**. After 30 min, the confocal microscopic images of RAW264.7 macrophages exhibited intense yellow-green fluorescence (Fig. 6(i)). The results suggested that probe **1** could be utilized to investigate endogenous hypochlorite in living cells.

3.6. Proposed mechanism for the reaction of probe *1* with HOCl

Zhang et al. reported [38] a rhodamine 6G hydrazide fluorescent chemosensor for detecting HOCl. The hydrazide moiety of the fluorescent probe might be oxidized by HOCl via an N-chlorination and subsequent HCl elimination pathway to release the fluorophore of rhodamine in the nucleophilic solvent.

To explore the sensing mechanism of **1** to ClO^- and determine the produced species, the reaction of **1** with 10 equiv. ClO^- was carried out in H_2O-DMSOsolution (v/v = 20/1), which was carried out by TLC and ESI-MS analysis. The formation of fluorescein as product was confirmed by comparison of R_f value with that of authentic fluorescein. The ESI mass spectra of the probe **1** solution before and after the addition of HOCl were illustrated in Figs. S4 and S5 (seeing ESI). The experimental results revealed that, with the presence of HOCl, the peak of probe **1** (*m*/*z* 429.1 $[M+H]^+$) disappeared, while three major new peaks emerged at *m*/*z* 621.58, 379.00 and 363.58, respectively. The three peaks represented the formation of intermediate oxide (**I**) and fluorescein (F) (*m*/*z* 621.58 $[I+2DMSO+H]^+$, 379.00 $[F+C_2H_5OH+H]^+$, 363.58 $[F+CH_3OH+H]^+$). Based on the ESI-MS results of the reaction products and TLC analyst, we proposed that the fluorescence off–on reaction process might proceed as the way depicted in Scheme 2.

Due to oxidation of sodium hypochlorite depends on pH value of the solution, catechol moiety reacted with sodium hypochlorite to form a higher concentration of chlorinated derivatives in lower or higher pH [35], which did not lead to open ring of spirolactam. It is agreement with Fig. 1. In the absence of ClO^-, probe **1** is colorless and nonfluorescent due to the closed spirolactam ring. In the presence of ClO^- (pH 6–8), the catechol moiety of probe **1** was oxidized to form open-ring intermediate M, and then the M further hydrolyzed to yellowish and strong fluorescent fluorescein in the presence of water (Scheme 3).

4. Conclusion

In summary, a new fluorescein-based fluorescence probe **1** for ClO^- has been synthesized and structurally characterized. Results show that it has a detection limit of 40 nM to hypochlorite anion. Moreover, most of background metal ions and anions showed small or no interference with the detection of ClO^-. In addition, it has favorable characteristics for biological imaging, including high water solubility, high fluorescence yield and biocompatibility. Confocal fluorescence microscopy imaging of RAW264.7 cells showed that the new probe **1** could be used as an effective fluorescent probe for detecting HOCl in living cells. We consider this sensor may prove to be a useful tool for investigating the roles of HOCl in biological and pathological processes.

Acknowledgments

We are grateful to financial support from the Jiangsu Key Laboratory of Industrial Water Conservation & Emission Reduction and the National Basic Research Program of China (973 Program, No. 2014CB846004) for financial support.

Appendix A. Supplementary data

Supplementary data related to this article can be found at http://dx.doi.org/10.1016/j.dyepig.2014.03.012.

References

[1] Gomes A, Fernandes E, Lima JL. Fluorescence probes used for detection of reactive oxygen species. J Biochem Biophys Methods 2005;65:45–80.
[2] Fiedler TJ, Davey CA, Fenna RE. X-ray crystal structure and characterization of halide-binding sites of human myeloperoxidase at 1.8 angstrom resolution. J Biol Chem 2000;275:11964–119671.
[3] Albrich JM, McCarthy CA, Hurst JK. Biological reactivity of hypochlorous acid – implications for microbicidal mechanisms of leukocyte myeloperoxidase. Proc Natl Acad Sci USA 1981;78:210–4.
[4] Chen XQ, Tian XZ, Shin I, Yoon J. Fluorescent and luminescent probes for detection of reactive oxygen and nitrogen species. Chem Soc Rev 2011;40:4783–804.
[5] Yuan L, Lin WY, Xie YN, Chen B, Song JZ. Fluorescent detection of hypochlorous acid from turn-on to FRET-based ratiometry by a HOCl-mediated cyclization reaction. Chem Eur J 2012;18:2700–6.
[6] Yuan L, Lin WY, Zheng KB, Zhu SS. FRET-based small-molecule fluorescent probes: rational design and bioimaging applications. Acc Chem Res 2013;46:1462–73.
[7] Chen XQ, Pradhan T, Wang F, Kim JS, Yoon J. Fluorescent chemosensors based on spiroring-opening of xanthenes and related derivatives. Chem Rev 2012;112:1910–56.
[8] Yang YM, Zhao Q, Feng W, Li FY. Luminescent chemodosimeters for bioimaging. Chem Rev 2013;113:192–270.
[9] Jin XL, Hao LK, Hu YL, She MY, Shi YN, Obst M, et al. Two novel fluorescein-based fluorescent probes for hypochlorite and its real applications in tap water and biological imaging. Sensors Actuat B 2013;186:56–60.
[10] Long LL, Zhang DD, Li XF, Zhang JF, Zhang C, Zhou LP. A fluorescence ratiometric sensor for hypochlorite based on a novel dual-fluorophore response approach. Anal Chim Acta 2013;775:100–5.
[11] Xie XL, Chen XP, Li B, Zhang LM. Study on a highly selective colorimetric chemosensor for Cu^{2+} detection and its indirect sensing for hypochlorite. Dyes Pigments 2013;98:422–7.
[12] Liu SR, Wu SP. Hypochlorous acid turn-on fluorescent probe based on oxidation of diphenyl selenide. Org Lett 2013;15:878–81.
[13] Liu F, Wu T, Cao JF, Zhang H, Hu MM, Sun SG, et al. A novel fluorescent sensor for detection of highly reactive oxygen species, and for imaging such endogenous hROS in the mitochondria of living cells. Analyst 2013;138:775–8.
[14] Wang BS, Li P, Yu FB, Song P, Sun XF, Yang SQ, et al. A reversible fluorescence probe based on Se-BODIPY for the redox cycle between HClO oxidative stress and H_2S repair in living cells. Chem Commun 2013;49:1014–6.
[15] Hou FJ, Zhang JJ, Yang YT, Chao JB, Yin CX, Zhang YB, et al. A fluorescein-based highly specific colorimetric and fluorescent probe for hypochlorites in aqueous solution and its application in tap water. Sensors Actuat B 2012;166–167:44–9.
[16] Koide Y, Urano Y, Hanaoka K, Terai T, Nagano T. Development of an Si–rhodamine-based far-red to near-infrared fluorescence probe selective for hypochlorous acid and its applications for biological imaging. J Am Chem Soc 2011;133:5680–2.
[17] Lou XD, Zhang Y, Li QQ, Qin JG, Li Z. A highly specific rhodamine-based colorimetric probe for hypochlorites: a new sensing strategy and real application in tap water. Chem Commun 2011;47:3189–91.
[18] Liu YL, Sun Y, Du J, Lv X, Zhao Y, Chen ML, et al. Highly sensitive and selective turn-on fluorescent and chromogenic probe for Cu^{2+} and ClO^- based on a *N*-picolinylrhodamine B-hydrazide derivative. Org Biomol Chem 2011;9:432–7.
[19] Cui K, Zhang DQ, Zhang GX, Zhu DB. A highly selective naked-eye probe for hypochlorite with the p-methoxyphenol-substituted aniline compound. Tetrahedron Lett 2010;51:6052–5.
[20] Yang YK, Cho HJ, Lee J, Shin I, Tae J. A rhodamine-hydroxamic acid-based fluorescent probe for hypochlorous acid and its applications to biological imagings. J Org Lett 2009;11:859–61.
[21] Panizzi P, Nahrendorf M, Wildgruber M, Waterman P, Figueiredo JL, Aikawa E, et al. Oxazine conjugated nanoparticle detects *in vivo* hypochlorous acid and peroxynitrite generation. J Am Chem Soc 2009;131:15739–44.
[22] Li GP, Zhu DJ, Liu Q, Xue L, Jiang H. A strategy for highly selective detection and imaging of hypochlorite using selenoxide elimination. Org Lett 2013;15:2002–5.
[23] Zhou Y, Li J, Chu K, Liu K, Yao C, Li J. ChemCommun 2012;48:4677–9.
[24] Xiong XQ, Song FL, Chen GW, Sun W, Wang JY, Gao P, et al. Construction of long-wavelength fluorescein analogues and their application as fluorescent probes. Chem Eur J 2013;19:6538–45.
[25] An JM, Yan MH, Yang ZY, Li TR, Zhou QX. A turn-on fluorescent sensor for Zn(II) based on fluorescein-coumarin conjugate. Dyes Pigments 2013;99:1–5.
[26] Kim HJ, Park JE, Choi MG, Ahn S, Chang SK. Selective chromogenic and fluorogenic signalling of Hg^{2+} ions using a fluorescein-coumarin conjugate. Dyes Pigments 2010;84:54–8.
[27] Duan Y, Liu M, Sun W, Wang M, Liu S, Li Q. Recent progress on synthesis of fluorescein probes. Mini Rev Org Chem 2009;6:35–43.
[28] Cook MP, Ando S, Koide K. One-step synthesis of a fluorescein derivative and mechanistic studies. Tetrahedron Lett 2012;53:5284–6.
[29] Haugland R, Spence M, Johnson I, Basey A. The handbook: a guide to fluorescent probes and labeling technologies. 10th ed. Carlsbad: Molecular Probes, Invitrogen Detection Technologies; 2005.
[30] Bernard V. Molecular fluorescence: principles and applications. Weinheim: Wiley-VCH VerlagGmbh; 2001.
[31] Kim HN, Zhiqian Guo ZQ, Zhu WH, Yoon J, Tian H. Recent progress on polymer-based fluorescent and colorimetric chemosensors. Chem Soc Rev 2011;40:79–93.
[32] Sun Z, Liu F, Chen Y, Tam PKH, Yang D. Org Lett 2008;10:2171–4.
[33] Jiang L, Wang L, Guo M, Yin G, Wang RY. Fluorescence turn-on of easily prepared fluorescein derivatives by zinc cation in water and living cells. Sensors Actuat B 2011;156:825–31.
[34] Magde D, Wong R, Seybold PG. Fluorescencequantum yields and their relation to lifetimes of rhodamine 6Gand fluorescein in nine solvents: improved absolute standards for quantum yields. Photochem Photobiol 2002;75:327–34.
[35] Kim T, Park S, Choi Y, Kim Y. A BODIPY-based probe for the selective detection of hypochlorous acid in living cells. Chem Asian J 2011;6:1358–61.
[36] Xiao YN, Zhang R, Ye ZQ, Dai ZC, An HY, Yuan JL. Lanthanide complex-based luminescent probes for highly sensitive time-gated luminescence detection of hypochlorous acid. Anal Chem 2012;84:10785–92.
[37] Michałowicz J, Duda W, Stufka-Olczyk J. Transformation of phenol, catechol, guaiacol and syringol exposed to sodium hypochlorite. Chemosphere 2007;66:657–63.
[38] Zhang Z, Zheng Y, Hang W, Yan XM, Zhao YF. Sensitive and selective off–on rhodamine hydrazide fluorescent chemosensor for hypochlorous acid detection and bioimaging. Talanta 2011;85:779–86.